

Production of Nonlinear SUSY Higgs Bosons at e^+e^- Colliders *

S.W. Ham¹, H. Genten², B.R. Kim², S.K. Oh¹

¹ Department of Physics, Kon-Kuk University, Seoul, Korea

² III. Physikalisches Institut, RWTH Aachen, Germany

Abstract

We investigate the Higgs sector of a nonlinear supersymmetric standard model at LEP 1 and LEP 2, as well as at future linear e^+e^- colliders with $\sqrt{s} = 500, 1000, \text{ and } 2000$ GeV. The LEP 1 data do not put any constraints on the parameters of the model, and allow a massless Higgs boson in particular. For LEP 2, there are remarkable differences between the Higgs productions at $\sqrt{s} = 175$ GeV on the one hand and that at $\sqrt{s} = 192$ GeV and 205 GeV on the other hand. The case for $\sqrt{s} = 175$ GeV is similar to LEP 1, whereas those for $\sqrt{s} = 192$ GeV and 205 GeV will be able to give experimental constraints on the parameters. Finally the e^+e^- colliders with $\sqrt{s} = 500, 1000, \text{ and } 2000$ GeV are most probably able to test the model conclusively.

* To be published in Physics Letters B. — This work is supported in part by the Ministry of Education, Korea, BSRI-96-2442.

1 Introduction

For more than a decade the phenomenology of supersymmetric models has been studied, and the search for supersymmetric particles is one of the main goals of existing and future accelerators. Most of the supersymmetric models investigated so far are linear ones, i.e., supersymmetry is realized linearly in them [1]. However, it is still an open question whether supersymmetry is realized linearly or nonlinearly.

The formalism for extending the standard model nonlinear-supersymmetrically was developed by Samuel and Wess [2]. Recently one of us has constructed the general form of a nonlinear supersymmetric standard model in curved space and derived the Higgs potential in the flat limit [3]. In global nonlinear supersymmetric models the only new particle is the Akulov-Volkov field [4], which is a Goldstone fermion. Experimentally, no Goldstino has been observed. In local nonlinear supersymmetric models this goldstino can be gauged away; it is absorbed into the gravitino, which becomes massive [5]. In the flat limit, the supergravity multiplet decouples from the ordinary matter with the only reminiscence of supersymmetry manifesting itself in the Higgs sector.

The Higgs sector of the nonlinear SUSY models is evidently larger than that of the Standard model. It contains at least two dynamical Higgs doublets and an auxiliary Higgs singlet. In the case that both a dynamical and an auxiliary singlet are included in the theory, the Higgs boson spectrum of the nonlinear model resemble that of the linear next-to-minimal supersymmetric standard model (NMSSM). In both models, there are three scalar Higgs bosons, two pseudoscalar Higgs bosons, and a pair of charged Higgs bosons. However, the structure of the Higgs potential is different between nonlinear and linear supersymmetry.

In this article we investigate the phenomenology of the nonlinear supersymmetric model with both an auxiliary and a dynamical Higgs singlet beside the doublets. In particular, we are interested in how far the Higgs sector can be tested at LEP, as well as at future e^+e^- colliders.

2 The Model

The complete Higgs potential of our model is given in Ref. [3]:

$$\begin{aligned}
 V = & \frac{1}{8}(g_1^2 + g_2^2)(|H^1|^2 - |H^2|^2)^2 + \frac{1}{2}g_2^2|H^{1+}H^2|^2 \\
 & + \mu_1^2|H^1|^2 + \mu_2^2|H^2|^2 + \mu_0^2|N|^2 \\
 & + \lambda_0^2|H^{1T}\epsilon H^2|^2 + k^2|N^\dagger N|^2 + |N|^2(\lambda_1^2|H^1|^2 + \lambda_2^2|H^2|^2) \\
 & + k\lambda_0[(H^{1T}\epsilon H^2)^\dagger N^2 + \text{h.c.}] \\
 & + [\lambda_1\mu_1|H^1|^2N + \lambda_2\mu_2|H^2|^2N + \lambda_0\mu_0(H^{1T}\epsilon H^2)^\dagger N + \text{h.c.}] \\
 & + [k\mu_0N^\dagger N^2 + \text{h.c.}] .
 \end{aligned} \tag{1}$$

The two Higgs doublets H^1 and H^2 and the singlet N develop vacuum expectation values v_1 , v_2 , and x , respectively. The full mass matrices can be found in

Ref. [3]. We denote the three scalar Higgs bosons and their masses respectively by S_1, S_2, S_3 and $m_{S_1} \leq m_{S_2} \leq m_{S_3}$. As in the case of the NMSSM [7], one can derive an upper bound on m_{S_1} in our model as

$$m_{S_1}^2 \leq m_{S_1, \max}^2 = m_Z^2 \left(\cos^2 2\beta + \frac{2\lambda_0^2}{g_1^2 + g_2^2} \sin^2 2\beta \right), \quad (2)$$

where $\tan \beta = v_2/v_1$. This relation shows that the quartic coupling λ_0 is relevant for the upper bound as in the case of the standard model. For $\lambda_0^2 \leq (g_1^2 + g_2^2)/2 = (0.52)^2$ this relation gives $m_{S_1}^2 \leq m_Z^2$, whereas for $\lambda_0^2 > (0.52)^2$ the upper bound is given by $m_{S_1}^2 \leq (1.92\lambda_0 m_Z)^2$. In the latter case, the upper bound of λ_0 determines that of m_{S_1} . For $m_t = 175$ GeV (190 GeV) and with the GUT scale as the cut-off scale, one obtains $\lambda_{0, \max} \approx 0.74$ (0.66) and $m_{S_1} \leq 130$ GeV (117 GeV).

It is very instructive to notice that, as in the case of the NMSSM [8], the upper bounds on m_{S_2} and m_{S_3} can be derived as functions of $m_{S_1, \max}$ and m_{S_1} :

$$\begin{aligned} m_{S_2}^2 \leq m_{S_2, \max}^2 &= \frac{m_{S_1, \max}^2 - R_1^2 m_{S_1}^2}{1 - R_1^2} \\ m_{S_3}^2 \leq m_{S_3, \max}^2 &= \frac{m_{S_1, \max}^2 - (R_1^2 + R_2^2) m_{S_1}^2}{1 - (R_1^2 + R_2^2)} \end{aligned} \quad (3)$$

with

$$\begin{aligned} R_1 &= U_{11} \cos \beta + U_{12} \sin \beta \\ R_2 &= U_{21} \cos \beta + U_{22} \sin \beta, \end{aligned} \quad (4)$$

where U_{ij} is the orthogonal matrix that diagonalises the scalar mass matrix, and $0 \leq R_1^2 + R_2^2 \leq 1$. Clearly, R_1 and R_2 are complicated functions of the relevant parameters. Nevertheless these relations turn out to be very useful to derive the lower limits on the production cross section of the scalar Higgs bosons.

3 Higgs Production at LEP 1 and LEP 2

The LEP 1 data yield an experimental lower bound of 60 GeV on the Higgs boson mass of the standard model, and 44 GeV for the mass of the lightest scalar Higgs boson of the minimal linear supersymmetric standard model (MSSM). In the case of the NMSSM the LEP 1 data do not exclude the existence of a massless scalar Higgs boson [9]. Now, we analyse the LEP 1 data in the frame of our model. As in the case of the NMSSM, the main contributions to the production cross section come from (i) the Higgs-strahlung process, (ii) the process where S_i is radiated off leptons or quarks, and (iii) associated pair production $P_j S_i$, where P_j ($j = 1, 2$) is a pseudoscalar Higgs boson:

$$\begin{aligned} \text{(i)} \quad Z &\rightarrow Z^* S_i \rightarrow \bar{f} f S_i \\ \text{(ii)} \quad Z &\rightarrow f \bar{f} \rightarrow \bar{f} f S_i \\ \text{(iii)} \quad Z &\rightarrow P_j S_i \rightarrow \bar{f} f S_i, \end{aligned} \quad (5)$$

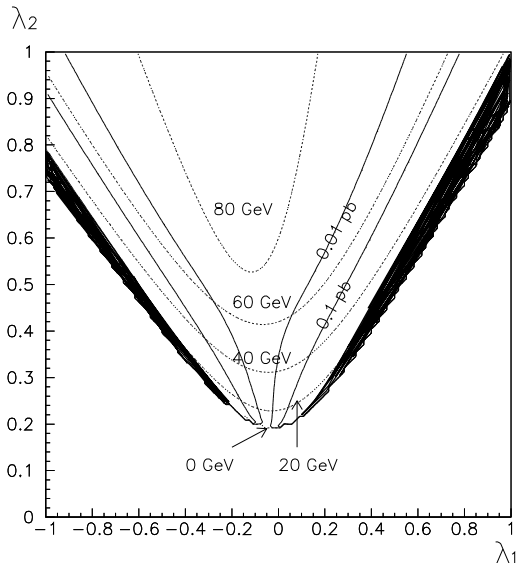


Figure 1: Contour lines of the lightest Higgs boson mass m_{S_1} (dotted) and of the production cross section σ_1 (solid) at $\sqrt{s} = m_Z$, as functions of λ_1 and λ_2 , for $\lambda_0 = 0.4$, $k = 0.02$, $\tan\beta = 3$, and $m_C = 200$ GeV. The shadowed region marks the parameter region excluded by LEP 1, defined as the region where the production cross section is greater than 1 pb.

The dominant contributions come from the b quark, $f = b$.

Our model has 6 free parameters which can be taken as $\lambda_0, k, \lambda_1, \lambda_2, \tan\beta$ and m_C (the charged Higgs mass). We search for parameter regions where none of S_i ($i = 1, 2, 3$) has enough production cross sections to be detected at LEP 1 and where $m_{S_1} = 0$ is still allowed. Fig. 1 shows such a region. We plot for $\lambda_0 = 0.4$, $k = 0.02$, $m_C = 200$ GeV, and $\tan\beta = 3$ the contours of m_{S_1} and the production cross section of S_1 , σ_1 . Only the shadowed region where $\sigma_1 \geq 1$ pb is excluded by the LEP 1 data. σ_2 is smaller than 12.3 fb and σ_3 vanishes in the entire plane. Thus we conclude that the LEP 1 data allow the existence of massless S_1 in our model.

Now we turn to LEP 2. In order to obtain a feeling we plot in Fig. 2a, 2b, and 2c the production sections of $\sigma_1^{(a)}$, $\sigma_2^{(a)}$, and $\sigma_3^{(a)}$ ($a = i, ii, iii$) for the three processes of Eq. (5), as well as the production cross sections σ_1 , σ_2 , and σ_3 for the sum of their processes, against the c.m. energy of the e^+e^- collider for a fixed set of parameters. The contribution from the Higgs-strahlung process is dominant for S_1 and S_2 . $\sigma_1^{(i)}$ and $\sigma_2^{(i)}$ are approximately equal to σ_1 and σ_2 , with $\sigma_1 > \sigma_1^{(i)}$ and $\sigma_2 > \sigma_2^{(i)}$, respectively. The dominant contribution of interferences between three processes arises positively at the Z peak for S_1 , negatively at $\sqrt{s} \approx 180$ GeV for S_2 , and negatively at $\sqrt{s} = 500$ GeV for S_3 . The maximum values of their contributions are ~ 1 fb for S_1 , $\sim 10^{-1}$ fb for S_2 , and $\sim 10^{-4}$ fb for S_3 . We observe that σ_2 is a very steep function of \sqrt{s} in the range between 150 GeV and 180 GeV, whereas it is rather flat between $\sqrt{s} = 180$ GeV and 240 GeV. Thus

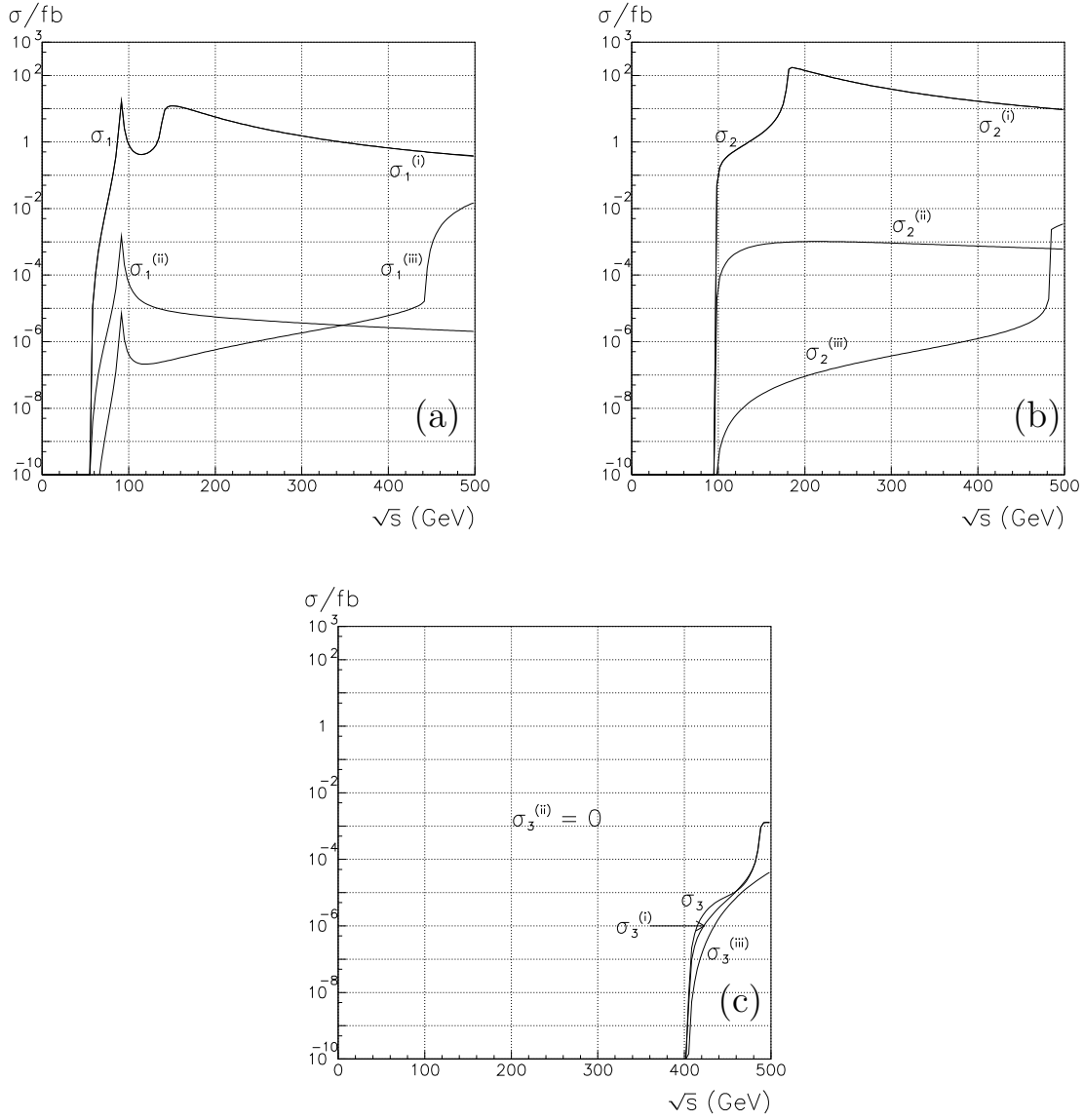


Figure 2: (a) The production cross sections $\sigma_1^{(a)}$ ($a = 1, 2, 3$) and σ_1 of S_1 for $\lambda_0 = 0.3$, $k = 0.02$, $\lambda_1 = -0.3$, $\lambda_2 = 0.45$, $\tan \beta = 6$, and $m_C = 400$ GeV. $\sigma_1^{(a)}$ and σ_1 denote the production cross sections for the three processes of Eq. (5) and for the sum of these processes, respectively. $\sigma_1^{(i)}$ is approximately equal to σ_1 . — (b) The according production cross sections of S_2 . $\sigma_2^{(i)}$ is approximately equal to σ_2 . — (c) The according production cross sections of S_3 . $\sigma_3^{(ii)}$ is negligible.

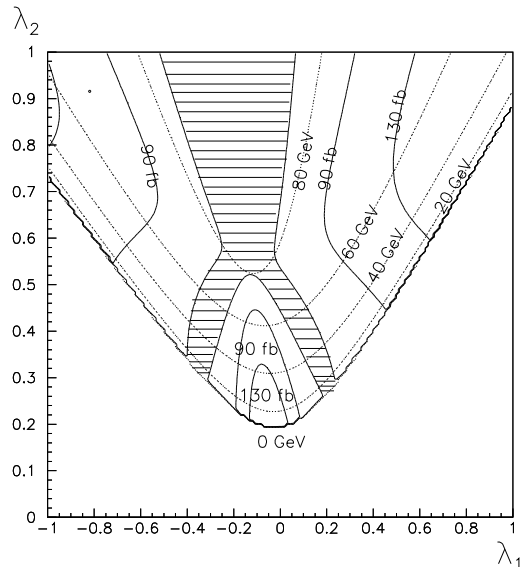


Figure 3: Contour lines of the lightest Higgs boson mass m_{S_1} (dotted) and of the production cross section $(\sigma_1 + \sigma_2)$ (solid) at $\sqrt{s} = 175$ GeV, as functions of λ_1 and λ_2 , for $\lambda_0 = 0.4$, $k = 0.02$, $\tan \beta = 3$, and $m_C = 200$ GeV. The cross section $(\sigma_1 + \sigma_2)$ is smaller than 50 fb in the hatched region.

we expect a relevant difference between the behavior at $\sqrt{s} = 175$ GeV on the one hand and that at $\sqrt{s} = 192$ GeV or 205 GeV on the other hand. It turns out that this expectation is generally correct when the sum $(\sigma_1 + \sigma_2)$ is around 30 fb \sim 50 fb. The discovery limit is about 50 fb for $m_S = 80$ GeV and 30 fb for $m_S = 40$ GeV at a luminosity of 500 pb^{-1} for $\sqrt{s} = 175$ GeV and at one of 300 pb^{-1} for $\sqrt{s} = 192$ and 205 GeV in our model [10]. In Fig. 3 the contours of m_{S_1} and those of $(\sigma_1 + \sigma_2)$ are plotted. We find $(\sigma_1 + \sigma_2) \leq 50$ fb and $(\sigma_1 + \sigma_2)_{\min} \approx 26$ fb in the hatched region. This region contains part of the $m_{S_1} = 0$ contour, which means that LEP 2 with $\sqrt{s} = 175$ GeV would not be able to put any constraints on m_{S_1} .

In order to see whether LEP 2 can put a constraint on the quartic coupling constant λ_0 , we scan the parameter space $|k| \leq 0.7$, $|\lambda_1| \leq 1$, $0 < \lambda_2 < 1$, $2 < \tan \beta < 15$, and $150 \text{ GeV} < m_C < 1000 \text{ GeV}$ and plot $(\sigma_1 + \sigma_2)$ as a function of λ_0 , for $\sqrt{s} = 175$ GeV in Fig. 4. About 10^6 points are considered. Again one sees that with a discovery limit of 30 fb \sim 50 fb LEP 2 with 175 GeV will not be able to put any experimental limit on λ_0 , either.

As expected, the situations both with $\sqrt{s} = 192$ GeV and with $\sqrt{s} = 205$ GeV are much more favorable. We scan the same parameter space as that of Fig. 4a and determine $(\sigma_1 + \sigma_2)$ as a function of λ_0 at these c.m. energies. We then plot the results in Fig. 4b for $\sqrt{s} = 192$ GeV and in Fig. 4c for 205 GeV. Fig. 4b shows that $(\sigma_1 + \sigma_2)$ is greater than 50 fb for $\lambda_0 \leq 0.54$. Thus LEP 2 with $\sqrt{s} = 192$ GeV would be able to put an experimental lower limit on λ_0 as

$$\lambda_{0,\text{EXP}} \geq 0.53. \quad (6)$$

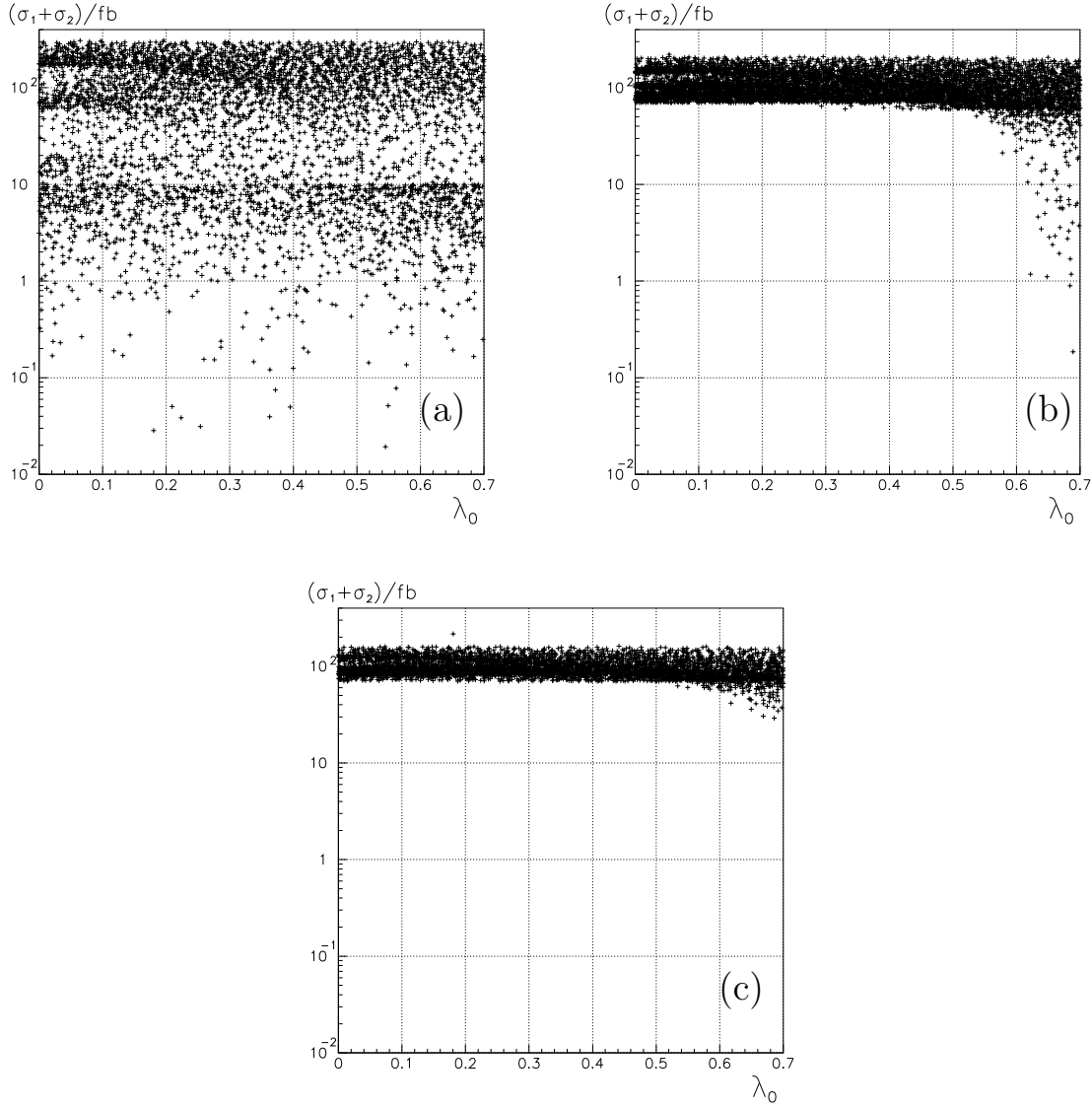


Figure 4: The cross section $(\sigma_1 + \sigma_2)$, as a function of λ_0 , for $|k| \leq 0.7$, $|\lambda_1| \leq 1$, $0 < \lambda_2 < 1$, $2 < \tan \beta < 15$, and $150 \text{ GeV} < m_C < 1000 \text{ GeV}$, at (a) $\sqrt{s} = 175 \text{ GeV}$, (b) $\sqrt{s} = 195 \text{ GeV}$, (c) $\sqrt{s} = 205 \text{ GeV}$.

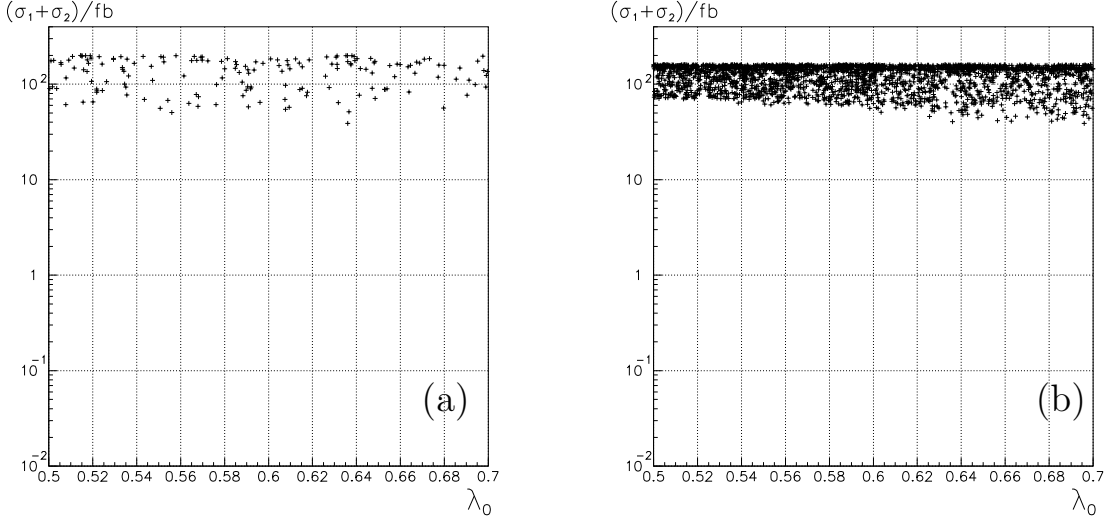


Figure 5: (a) The cross section $(\sigma_1 + \sigma_2)$ with $m_{S_1} \leq 10$ GeV at $\sqrt{s} = 192$ GeV, as function of λ_0 , for $|k| \leq 0.7$, $|\lambda_1| \leq 1$, $0 < \lambda_2 < 1$, $2 < \tan\beta < 15$, and 150 GeV $< m_C < 1000$ GeV. — (b) The same as (a), except for $\sqrt{s} = 205$ GeV and $m_{S_1} \leq 27$ GeV.

This experimental lower limit implies via Eq. (2) an experimental lower limit on the upper limit on m_{S_1} as

$$m_{S_1, \text{max,EXP}} \geq 1.92 \cdot \lambda_{0, \text{EXP}} \cdot m_Z \approx 92 \text{ GeV} . \quad (7)$$

Similarly from Fig. 4c we conclude for $\sqrt{s} = 205$ GeV

$$\lambda_{0, \text{EXP}} \geq 0.61 \quad (8)$$

and

$$m_{S_1, \text{max,EXP}} \geq 107 \text{ GeV} . \quad (9)$$

Now, we turn to the question of imposing a lower limit on m_{S_1} itself. In Fig. 5a we plot $(\sigma_1 + \sigma_2)$ for $\sqrt{s} = 192$ GeV with the constraint $m_{S_1} \leq 10$ GeV. We omit the points for $\lambda_0 < 0.5$ as in the region $(\sigma_1 + \sigma_2) \geq 50$ fb. For $m_{S_1} \geq 10$ GeV + 1 GeV = 11 GeV, there are points with $(\sigma_1 + \sigma_2) < 30$ fb. We find that $(\sigma_1 + \sigma_2)$ for $m_{S_1} < 10$ GeV is always greater than 30 fb. This implies that LEP 2 with $\sqrt{s} = 192$ GeV and discovery limit 30 fb would be able to put an experimental lower limit on m_{S_1} as

$$m_{S_1, \text{EXP}} \geq 10 \text{ GeV} . \quad (10)$$

In Fig. 5b we plot the same as in 5a for $\sqrt{s} = 205$ GeV. In this case we obtain

$$m_{S_1, \text{EXP}} \geq 27 \text{ GeV} . \quad (11)$$

4 Higgs Production at LC 500, 1000, and 2000

As discussed in section 2, the upper bound of m_{S_1} is about 130 GeV. Thus, if the collider energy \sqrt{s} is larger than $E_C = m_Z + 130$ GeV, which is a kind of threshold energy, the production via the Higgs-strahlung is possible in the whole parameter space for at least one of S_i ($i = 1, 2, 3$). In this case one should consider the productions of S_1, S_2 , and S_3 simultaneously. In order to be systematic, we consider the production cross sections of S_1, S_2 , and S_3 via the Higgs-strahlung process, denoted respectively by σ_1, σ_2 , and σ_3 :

$$\begin{aligned}\sigma_1(m_{S_1}) &= \sigma_{\text{SM}}(m_{S_1})R_1^2 \\ \sigma_2(m_{S_2}) &= \sigma_{\text{SM}}(m_{S_2})R_2^2 \\ \sigma_3(m_{S_3}) &= \sigma_{\text{SM}}(m_{S_3})(1 - R_1^2 - R_2^2),\end{aligned}\tag{12}$$

where $\sigma_{\text{SM}}(m)$ is the cross section in the standard model for the production of the Higgs boson of mass m via the Higgs-strahlung process.

A useful observation is that $\sigma_i(m_{S_i, \text{max}}) \leq \sigma_i(m_{S_i})$, which allows to derive the parameter-independent lower limit of σ_i as we will show in the following. At first, we determine the cross sections $\sigma_1(R_1, R_2, m_{S_1})$, $\sigma_2(R_1, R_2, m_{S_2, \text{max}})$, and $\sigma_3(R_1, R_2, m_{S_3, \text{max}})$ at a fixed set of m_{S_1} , R_1 , and R_2 . Secondly, we keep R_1 and R_2 fixed, while varying m_{S_1} from its minimum to maximum and determine the quantity

$$\sigma(R_1, R_2) = \min[\max(\sigma_1, \sigma_2, \sigma_3)] \quad (0 \leq m_{S_1} \leq m_{S_1, \text{max}})\tag{13}$$

where $\sigma_1 = \sigma_1(R_1, R_2, m_{S_1})$ and $\sigma_i = \sigma_i(R_1, R_2, m_{S_i, \text{max}})$ ($i = 2, 3$).

As last step, we vary R_1^2 and R_2^2 from 0 to 1 ($0 \leq R_1^2 \leq 1$ and $0 \leq R_2^2 \leq 1$) and plot $\sigma(R_1, R_2)$ in the R_1^2 - R_2^2 plane. For $\sqrt{s} \leq E_T = m_Z + m_{S_1, \text{max}} \approx 222$ GeV this plot produces null results because $\sigma(R_1, R_2) = 0$, which is the case for LEP 2. For $\sqrt{s} > E_T$, $\sigma(R_1, R_2)$ never vanishes in the entire R_1^2 - R_2^2 plane and the minimum value of $\sigma(R_1, R_2)$ is a parameter-independent lower limit of one of $\sigma_1, \sigma_2, \sigma_3$. Thus, this minimum is a characteristic quantity of the model.

In Fig. 6a we plot $\sigma(R_1, R_2)$ for $\sqrt{s} = 500$ GeV. The minimum of $\sigma(R_1, R_2)$ in the plane is about 19 fb, which means that one of S_i will be produced with $\sigma_i \geq 19$ fb for $\sqrt{s} = 500$ GeV. For a discovery limit of 50 events per year one would need an integrated luminosity of about 2.5 fb^{-1} , which is a realistic one.

Fig. 6b and 6c show $\sigma(R_1, R_2)$ for $\sqrt{s} = 1000$ GeV and 2000 GeV, respectively. The minimum $\sigma(R_1, R_2)$ is about 5 fb for $\sqrt{s} = 1000$ GeV and 1.2 fb for $\sqrt{s} = 2000$ GeV. The conclusion is that this model may most probably be tested at future LC 500, 1000, and 2000 colliders.

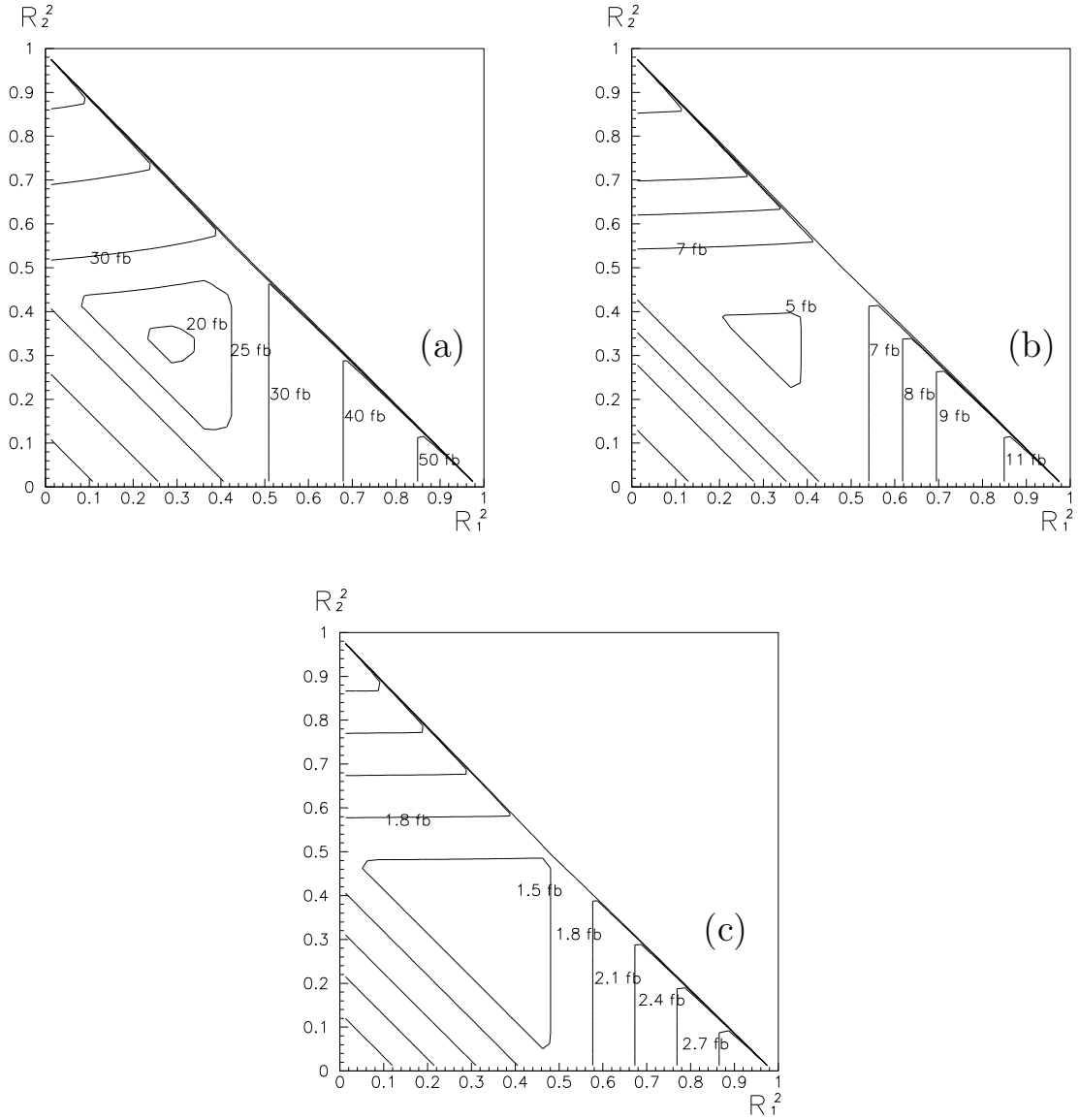


Figure 6: Contour lines of $\sigma(R_1, R_2)$ as defined by Eq. (13) for (a) $\sqrt{s} = 500$ GeV, (b) $\sqrt{s} = 1000$ GeV, (c) $\sqrt{s} = 2000$ GeV. The minimum values are 19 fb for (a), 5 fb for (b), and 1.2 fb for (c).

5 Qualitative Discussion about Decay Modes

The main purpose of the present paper is to investigate at which energy and luminosity our model could in principle be tested. This is what we have just done considering the production of on-shell S_i . However, for experimental searches, more detailed informations are needed, in particular on their decay modes. Comprehensive investigations in this respect are under way, similar to the investigations done for the MSSM [11]. Here, we merely make a few quantitative remarks.

The dominant decay modes of S_1 are those into b quark and τ lepton pairs, except for the case where m_{S_1} approaches its maximum value. In this case, S_1 behaves like the standard model Higgs boson, and other decay modes, for example those into pairs of gauge bosons will become important, with partial widths that could become comparable to those of the $b\bar{b}$ channel for large $\tan\beta$. An important signature of S_1 is certainly its upper mass bound of about 130 GeV.

The decay modes of the heavy bosons S_2 , S_3 could be more complex, depending on $\tan\beta$. For large $\tan\beta$ these bosons decay dominantly to $b\bar{b}$ and $\tau^+\tau^-$. In the MSSM, the decay of the heavy neutral scalar Higgs boson into a pair of light scalar or pseudoscalar bosons can be dominant in the parameter region where the mass of the heavy Higgs boson approaches its maximum [11]. The question whether this could happen in our model, too, is under investigation. For small $\tan\beta$, the decay modes into pairs of light Higgs bosons, gauge boson pairs, and mixed pairs of Higgs and gauge bosons will become important. Above the $t\bar{t}$ threshold, S_3 will decay dominantly into t quark pairs. The upper bound of m_{S_2} is smaller than the threshold. We numerically determined bounds for the masses of S_2 , S_3 , P_1 , and P_2 by systematically scanning the parameter space and obtained $55 \text{ GeV} \lesssim m_{S_2} \lesssim 260 \text{ GeV}$, $m_{S_3} \gtrsim 150 \text{ GeV}$, $m_{P_1} \lesssim 240 \text{ GeV}$, and $m_{P_2} \gtrsim 120 \text{ GeV}$.

Another interesting question is how to distinguish the Higgs sector of our model from those of other models, in particular, from that of the NMSSM, which has the same Higgs particle spectrum. The Higgs sectors should be easy to distinguish if some of the s-particles of the NMSSM were light enough for the Higgs bosons to decay into. Otherwise, the decay patterns should be very similar in both models. A theoretical possibility to distinguish the models arises from the number of free parameters of the Higgs sector. Although both models have the same number of parameters on tree level, the numbers differ on loop level. For the NMSSM, the number increases due to the contributions of the s-particles, whereas for our model, it remains the same, i.e. six. So once all Higgs bosons were found, our model could be determined completely by six independent experiments.

6 Conclusion

We demonstrated that at LEP 2 with $\sqrt{s} = 175 \text{ GeV}$ no bounds on m_{S_1} and λ_0 can be derived, whereas LEP 2 with $\sqrt{s} = 192 \text{ GeV}$ and $\sqrt{s} = 205 \text{ GeV}$ will be

able to put experimental lower bounds on λ_0 , $m_{S_1, \max}$, and m_{S_1} . Our analysis predicts

$$\begin{aligned}
 \lambda_{0, \text{EXP}} &\geq 0.53 \text{ (0.61)} \\
 m_{S_1, \max, \text{EXP}} &> 92 \text{ GeV (107 GeV)} \\
 m_{S_1, \text{EXP}} &> 10 \text{ GeV (27 GeV)}
 \end{aligned}
 \tag{14}$$

for $\sqrt{s} = 192 \text{ GeV (205 GeV)}$. We also derived a lower limit of the production cross sections of the scalar Higgs bosons to be 19 fb, 5 fb and 1.2 fb at e^+e^- colliders with $\sqrt{s} = 500 \text{ GeV, 1000 GeV, and 2000 GeV}$ respectively, which are large enough to test the model conclusively.

One should remark that the above results are based on tree level calculations.

References

- [1] P. Fayet and S. Ferrara, Phys. Rep. **32** (1977) 249; H.P. Nilles, Phys. Rep. **110** (1984) 1; H.E. Haber and G.L. Kane, Phys. Rep. **117** (1985) 75; A.B. Lahanes and D.V. Nanopoulos, Phys. Rep. **145** (1991) 1; R. Barbieri, Riv. Nuovo Cimento **11** (1988) 1.
- [2] S. Samuel and J. Wess, Nucl. Phys. **B233** (1984) 488; **B226** (1983) 289.
- [3] B. R. Kim, Z. Phys. **C67** (1995) 337.
- [4] D. V. Volkov and V. P. Akulov, Phys Lett. **B46** (1973) 109.
- [5] S. Deser and B. Zumino, Phys Rev. Lett **38** (1977) 1433; D.Z. Freedman and A. Das, Nucl. Phys **B120** (1977) 221.
- [6] J. Ellis, J. F. Gunion, H. E. Haber, L. Roszkowski and F. Zwirner, Phys. Rev. **D39** (1989) 844.
- [7] M. Drees, Int. J. Mod. Phys. **A4** (1989) 3635.
- [8] J.R. Espinosa and M. Quirós, Phys Lett **B279** (1992) 92; Phys Lett **B302** (1993) 51; G. Kane, C. Kolda and J.D. Wills, Phys. Rev. Lett. **70** (1993) 2686; J. Kamoshita, Y. Okada and M. Tanaka, Phys. Lett. **B328** (1994) 67; S.F. King and P.L. White, SHEP-95-27, hepdata reports OUTP-95-319, to appear in Phys. Rev. **D**.
- [9] B.R. Kim, S.K. Oh and A. Stephan, Proceedings of e^+e^- Collisions at 500 GeV, The Physics Potential, DESY 92-123B (1992) 697.
- [10] P. Janot, Private communication.
- [11] A. Djouadi, J. Kalinowski and P.M. Zerwas, DESY 95-211, KA-TP-9-95, IFT-95-14 (1995).